Laser-assisted Compton scattering of x-ray photons

D. Seipt[1,2,*] and B. Kämpfer[2,3]
[1]*Helmholtz-Institut Jena, Fröbelstieg 3, 07743 Jena, Germany*
[2]*Helmholtz-Zentrum Dresden-Rossendorf, P.O. Box 510119, 01314 Dresden, Germany*
[3]*Institut für Theoretische Physik, Technische Universität Dresden, 01062 Dresden, Germany*
(Received 9 September 2013; published 28 February 2014)

The Compton scattering of x-ray photons, assisted by a short intense optical laser pulse, is discussed. The differential scattering cross section reveals the interesting feature that the main Klein-Nishina line is accompanied by a series of side lines forming a broad plateau where up to $O(10^3)$ laser photons participate simultaneously in a single scattering event. An analytic formula for the width of the plateau is given. Due to the nonlinear mixing of x-ray and laser photons a frequency-dependent rotation of the polarization of the final-state x-ray photons relative to the scattering plane emerges. A consistent description of the scattering process with short laser pulses requires to work with x-ray pulses. An experimental investigation can be accomplished, e.g., at LCLS or the European XFEL, in the near future.

DOI: 10.1103/PhysRevA.89.023433 PACS number(s): 32.80.Wr, 34.80.Qb, 41.60.Cr

I. INTRODUCTION

Compton scattering [1], i.e., the scattering of x or γ rays off free electrons is one of the fundamental interaction processes of photons with charged particles. A particular feature is the dependence of the frequency ω'_{KN} of the scattered photon on the angle ϑ, $\omega'_{\mathrm{KN}} = \omega_X/(1 + \frac{\omega_X}{m}[1 - \cos\vartheta])$, in the initial rest frame of the scattering particle with mass m. For linearly polarized x rays the scattered photon polarization direction is the same as for electric dipole radiation. These properties become modified in laser-assisted Compton scattering $X + L + e \to e' + X'$, where we suppose alignment of the x-ray beam [X, frequency $\omega_X \sim O(\mathrm{keV})$] and an intense optical laser pulse [L, frequency $\omega_L \sim O(\mathrm{eV})$]. The frequency ω' of the scattered photon X' in the initial rest frame of the electron e reads (with $\hbar = c = 1$)

$$\omega'(\ell,\vartheta) = \frac{\omega_X + \ell\omega_L}{1 + \frac{\omega_X + \ell\omega_L}{m}(1 - \cos\vartheta)}\,. \tag{1}$$

That means a nonlinear frequency mixing occurs with ℓ parametrizing the amount of energy and momentum absorbed from the laser field in the scattering process. The quantity ℓ can be related to the number of involved laser photons, in particular in the limit of infinite monochromatic plane waves, where the values of ℓ become discrete ℓ_N, with integers N referring to the number of exchanged laser photons (see Appendix for details). The value of ℓ may be positive or negative, leading to the formation of side bands in the energy spectrum [2]. A similar effect has been observed also for laser-assisted atomic processes [3,4]. Obviously, $\ell = 0$ recovers the laser-free scattering of an x-ray photon with known Klein-Nishina (KN) kinematics. A large frequency ratio $\varkappa = \omega_X/\omega_L$ leads to a strong dynamical enhancement of nonlinear multilaser photon effects such that many side lines form a broad plateau reaching to $|\ell| \gg 1$. Although the possibility of a strong enhancement was recognized in Ref. [2], the shape of the spectrum in frequency space and the cutoff values of ℓ, in particular their angular dependencies, have never been calculated precisely to the best of our knowledge. This gap will be filled in this paper, where we calculate the frequency spectrum and provide a formula for the angular dependence of the cutoff energies of the side-band plateau.

Observing the plateau of side lines within a certain frequency interval determined by cutoff values with special angular dependencies is a clear experimental signal for laser-assisted Compton scattering of x rays, i.e., a new possibility to observe $O(10^3)$ multiphoton effects in strong-field QED. In addition, as we shall show below, the polarization properties of X' represent a new feature. The nonlinear frequency mixing leads to a frequency-dependent rotation of the polarization of the final-state photons. This rotation does not affect the main KN line ($\ell = 0$) and is useful to identify the side bands in an experiment.

The basic scattering process can be understood qualitatively in a classical picture, where the slow electron motion due to the laser is described classically. For high-intensity laser fields of the order of 10^{18} W/cm^2 the motion of electrons becomes relativistic and nonlinear, resembling a figure-eight motion with a velocity component in the laser beam direction [5,6], superimposed to the usual transverse motion. In this picture, laser-assisted Compton scattering corresponds to the scattering of x rays off accelerated charges, and the broadening of the KN line occurs due to a time-dependent Doppler shift induced by the figure-eight motion.

In our approach we fully take into account the finite lengths of both the x-ray and laser pulses, going beyond infinite monochromatic plane wave approximation [2,7–13] or the limit of long laser pulses and infinite x-ray waves [14]. Pulse shape effects have been recently proved to have a significant impact of the scattering spectra in nonlinear Compton scattering [15–21], pair production [22–25], and other strong-field QED processes [6,26].

Taking into account the finite pulse length is necessary as we envisage a specific experimental setup involving a petawatt class optical laser in combination with an x-ray free electron laser, which both produce short femtosecond light pulses. In some previous papers, relations for the cross section were calculated either for small numbers of exchanged laser photons N [7–9], or they were limited to nonrelativistic intensities

*d.seipt@gsi.de

[2], or were restricted to the discussion of energy-integrated angular distributions [10]; the partial cross sections have been calculated for arbitrary values of N in terms of generalized Bessel functions, e.g., in Ref. [11].

Our paper is organized as follows. In Sec. II we formulate the matrix element for photon emission in the combined x-ray and laser fields and discuss the physical significance of the various terms occurring in a weak-field expansion in the x-ray field. In Sec. III the leading-order contribution in the x-ray field is evaluated and used to calculate an expression for the cross section for laser-assisted Compton scattering. The essential properties of the photon spectrum are discussed in Sec. IV where we present results for the differential cross section as well as the final photon polarization for a representative set of parameters. High-order multiphoton effects are quantified via an analytic formula for the cutoff values of the frequency spectrum. We discuss and summarize our results in Sec. V where we also address some aspects of an experimental realization. Appendix provides a brief discussion on the limit of infinitely long plane waves.

II. MATRIX ELEMENT

We describe the photon beams as a classical plane wave background field with four-vector potential $A^\mu = A_X^\mu(\varkappa\phi) + A_L^\mu(\phi)$, defining $\phi = k_L\cdot x \equiv k_L^\mu x_\mu$ with $k_L^\mu = (\omega_L, \boldsymbol{k}_L)$ and $k_X^\mu = \varkappa k_L^\mu$. We consider orthogonal linear polarizations, $A_X\cdot A_L = 0$. The vector potentials are parametrized as $A_j^\mu(\phi) = \frac{ma_j}{e}\epsilon_j^\mu g_j(\phi)\cos\phi$, $j\in\{X,L\}$, with the modulus of the electron charge e, normalized polarization vectors ϵ_j^μ and invariant laser strength parameters a_j. We emphasize the appearance of the envelope functions g_j accounting for the finite pulse lengths T_j of both the x-ray and the laser pulses, which are assumed to be synchronized temporally.

For the given background field A^μ we may work in the Furry picture employing Volkov states [6,27]

$$\Psi_p(x,A) = e^{-ip\cdot x - \frac{i}{2k_L\cdot p}\int^\phi d\phi'[2ep\cdot A(\phi') - e^2A^2(\phi')]} \times\left(1+\frac{e\not{k}_L\not{A}}{2k_L\cdot p}\right)u_p\,, \tag{2}$$

as nonperturbative solutions of the Dirac equation $(i\partial\!\!\!/ - e\not{A} - m)\Psi_p(x) = 0$. The free Dirac spinors u_p fulfill $(\not{p}-m)u_p = 0$ and are normalized to $\bar{u}_p u_p = 2m$. Moreover, Feynman's slash notation $\not{p} = \gamma_\mu p^\mu$ is employed.

The S matrix for the emission of the photon X' with momentum k' is given by

$$S = -ie\int d^4x\,\bar{\Psi}_{p'}(x,A)\not{\epsilon}'e^{ik'\cdot x}\Psi_p(x,A), \tag{3}$$

as depicted in Fig. 1(a). The nonperturbative expression (3), in both a_X and a_L, is correct for arbitrary x-ray and laser intensities, describing multiphoton processes for both the laser and x-ray field. For instance, in the papers [8,28–31] situations have been discussed where it is necessary to treat both field on equal footing. However, even for present XFEL technology $a_X \ll 1$, and we may expand the S matrix into a power series in a_X to get

$$S = S_0 + a_X(S_{+1}+S_{-1}) + O\left(a_X^2\right). \tag{4}$$

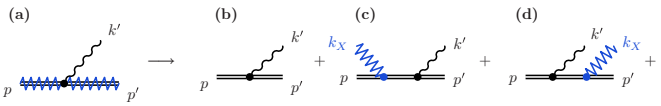

FIG. 1. (Color online) Expansion of the Feynman diagram (a) for photon emission off a dressed electron (double zigzag line: electron in the combined laser and x-ray field, plain double line: electron in the laser background, wavy line: photon, and zigzag line: x-ray) for a weak x-ray field in powers of a_X, yielding spontaneous emission (b), laser-assisted Compton scattering (c) and induced emission (d).

This corresponds to treating the field A_X as a perturbation, going to a single x-ray photon approximation. A similar technique of expanding a Volkov wave function in a weak field has also been used, e.g., in Refs. [12,13,32,33]. Here, we first discuss the physical implications of that expansion and give an interpretation for the individual terms of Eq. (4). Details of the derivation are presented in the next section.

The lowest-order term $S_0 \propto a_X^0$ [see Fig. 1(b)] corresponds to nonlinear optical-laser Compton scattering without any participation of x-ray photon [34]. This scattering of laser photons off free electrons is named commonly nonlinear Thomson or Compton scattering, see, e.g., Refs. [15–19,35–37]. In the classical picture, this is the radiation due to the accelerated figure-eight motion of the electron in the laser. In the present context it may be dubbed spontaneous emission. Using moderately strong laser pulses with $a_L \sim 1$, the nonlinear interaction with more than one photon has been verified experimentally [38–40] via the observation of harmonic radiation. In these experiments, only a rather small number of $O(2$–$5)$ laser photons was participating in a single scattering event.

The leading-order process involving x-ray photons is proportional to a_X^1 and consists of two terms which correspond to the absorption [S_{+1}, Fig. 1(c)] or the emission [S_{-1}, Fig. 1(d)] of a single x-ray photon from or to the initial beam. The laser-assisted Compton scattering is described by S_{+1} with the formal energy-momentum conservation

$$p + k_X + \ell k_L = p' + k'\,, \tag{5}$$

which arises upon the integration in (3) together with introducing the auxiliary variable ℓ; note that one still has to integrate over ℓ, therefore (5) has only three independent conservation laws for the light-front components [16,19]

$$\boldsymbol{p}^\perp = \boldsymbol{p}'^\perp + \boldsymbol{k}'^\perp, \quad p^- = p'^- + k'^-\,. \tag{6}$$

The light front is defined with respect to k_L such that $k_L^+ = 2\omega_L$ is the only nonvanishing light-front component of k_L and $\phi = \omega_L x^-$ becomes the light-front time-evolution parameter. By adopting a coordinate system in which the laser propagates in the z direction the light-front components of any four-vector read $x^\pm = x^0 \pm x^3$ and $\boldsymbol{x}^\perp = (x^1, x^2)^T$.

The fourth condition in (5), $p^+ + k_X^+ + \ell k_L^+ = p'^+ + k'^+$, furnishes a relation between the frequency ω' and the variable ℓ via Eq. (1). This may also be turned around expressing ℓ as a function of k' via

$$\ell(\omega',\vartheta) = \frac{k'\cdot p - k_X\cdot(p-k')}{k_L\cdot(p-k')}\,. \tag{7}$$

Thus, one can chose any of the two quantities ω' or ℓ to be the independent variable defining the other one. The lower limit of ℓ is determined by the condition $\omega' \geqslant 0$, yielding $\ell \geqslant -\varkappa$.

The meaning of ℓ is that it parametrizes the amount of laser four-momentum k_L absorbed in the scattering process and it is the Fourier conjugate to the laser phase ϕ [22,41]. It can be considered as a continuous analog of the photon number encountered for infinite monochromatic plane wave fields [41,42], cf. also Appendix.

Due to the large frequency ratio the two partial processes (b) and (c) are separated kinematically: While photons from spontaneous emission S_0 have typical energies of $\omega' = O(\text{eV})$ [Eq. (1) with $\omega_X = 0$], the photons from laser-assisted Compton scattering S_{+1} are $\omega' = O(\text{keV})$. The induced process S_{-1}, related to double Compton scattering [43–45], is strongly suppressed here in the keV frequency range due to the large value of $\varkappa$.

III. CROSS SECTION FOR LASER-ASSISTED COMPTON SCATTERING

Here we present the derivation of the matrix element for laser-assisted Compton scattering S_{+1}, which is needed to calculate the corresponding cross section. To this end we have to linearize expression (3) in a_X and extract the part representing the absorption of an x-ray photon from the field A_X, i.e., a process with the formal energy momentum conservation (5). For these purposes it is convenient to split the integrand of S in Eq. (3) into the pre-exponential term $\Gamma(x) = (1 + \frac{e\not{A}\not{k}_L}{2k_L\cdot p'})\not{\epsilon}'(1 + \frac{e\not{k}_L\not{A}}{2k_L\cdot p})$ and a phase factor $F(x) = (p' + k' - p)\cdot x - \int d\phi\,(\frac{ep\cdot A(\phi)}{k_L\cdot p} - \frac{ep'\cdot A(\phi)}{k_L\cdot p'}) + (\frac{e^2}{2k_L\cdot p} - \frac{e^2}{2k_L\cdot p'})\int d\phi\, A^2(\phi)$, such that

$$S = -ie\int d^4x\,\bar{u}_{p'}\Gamma(x)u_p e^{iF(x)}\,, \tag{8}$$

where terms proportional to a_X^2 both in the exponent F and the pre-exponential Γ can be dropped by virtue of $a_X \ll 1$. We need to linearize furthermore the phase exponent according to

$$e^{iF} \approx e^{iF_0 + iF_X} \approx e^{iF_0}(1 + iF_X)\,, \tag{9}$$

where F_0 is the part of the phase of S independent of A_X, i.e., $\propto a_X^0$, and

$$F_X = \alpha_X \int d(\varkappa\phi)\, g_X(\varkappa\phi)\cos(\varkappa\phi) \tag{10}$$

is linear in a_X with

$$\alpha_X = ma_X\left(\frac{\epsilon_X\cdot p'}{k_X\cdot p'} - \frac{\epsilon_X\cdot p}{k_X\cdot p}\right). \tag{11}$$

Multiplying with the pre-exponential we obtain up to linear order in a_X

$$\Gamma e^{iF} \approx \Gamma_0 e^{iF_0} + (\Gamma_X + iF_X\Gamma_0)\,e^{iF_0}\,, \tag{12}$$

where $\Gamma_0 = \sum_{n=0}^{2} V_n^L[g_L(\phi)\cos\phi]^n$ is independent of A_X, and $\Gamma_X = V_1^X g_X(k_X\cdot x)\cos k_X\cdot x$ is linear in a_X. The pre-exponential coefficients are defined by

$$V_0^j = \not{\epsilon}'\,, \tag{13}$$

$$V_1^j = ma_j\left(\frac{\not{\epsilon}_j\not{k}_j\not{\epsilon}'}{2k_j\cdot p'} + \frac{\not{\epsilon}'\not{k}_j\not{\epsilon}_j}{2k_j\cdot p}\right), \tag{14}$$

$$V_2^j = \frac{m^2a_j^2\,\epsilon'\cdot k_j}{2p\cdot k_j\, p'\cdot k_j}\not{k}_j, \tag{15}$$

where $j \in (X,L)$ as above. In expression (12), the first term gives rise to S_0 and the second term is $\propto a_X$ and contains both $S_{\pm1}$, since the real field A_X contains both the amplitudes for photon absorption and emission. Having linearized the expressions in A_X we may now go over to a complex field via $\cos(k_X\cdot x) = (e^{ik_X\cdot x} + e^{-ik_X\cdot x})/2 \to e^{-ik_X\cdot x}/2$, selecting only the amplitude for an x-ray photon in the initial channel, yielding

$$S_{+1} \propto \tfrac{1}{2}\big(V_1^X g_X - \alpha_X\Gamma_0 G_X\big)e^{iF_0 - ik_X\cdot x} \tag{16}$$

with $G_X = -ie^{i\varkappa\phi}\int^{\varkappa\phi} d\tau\, g_X(\tau)e^{-i\tau}$ and α_X defined in (11). Employing the slowly varying envelope approximation (see, e.g., Ref. [18]) for the x-ray pulse means $G_X \to g_X$. Physically, this approximation means neglecting a spatial displacement of the electron due to the action of the x-ray field. The order of magnitude of this effect is given by $1/\omega_X T_X$, which is much smaller than unity for femtosecond x-ray pulses of several keV frequencies.

Performing the space-time integrations in (8), the matrix element S_{+1} for laser-assisted Compton scattering can be written as

$$S_{+1} = -4ie\pi^3\int d\ell\,\delta^{(4)}(p + \ell k_L + k_X - p' - k')M(\ell) \tag{17}$$

with the amplitude

$$M(\ell) = \bar{u}_{p'}\left[V_1^X C_0(\ell) - \alpha_X\sum_{n=0}^{2} V_n^L C_n(\ell)\right]u_p. \tag{18}$$

and the coefficients V_n^j defined in (13)–(15). The functions C_n in (18) are given by

$$C_n = \int_{-\infty}^{\infty} d\phi\,[g_L(\phi)\cos\phi]^n g_X(\varkappa\phi)e^{i\int^{\phi} d\phi'\psi(\phi')} \tag{19}$$

with the dynamic phase

$$\psi(\phi) = \ell + \alpha_L g_L(\phi)\cos\phi + \beta_L[g_L(\phi)\cos\phi]^2 \tag{20}$$

having defined

$$\alpha_L = ma_L\left(\frac{\epsilon_L\cdot p'}{k_L\cdot p'} - \frac{\epsilon_L\cdot p}{k_L\cdot p}\right) \tag{21}$$

and

$$\beta_L = \frac{m^2a_L^2}{2}\left(\frac{1}{k_L\cdot p'} - \frac{1}{k_L\cdot p}\right). \tag{22}$$

Upon performing the integration over $d\ell$ in (17) the argument of the amplitude M becomes a function of ω' and ϑ, i.e., $M(\ell(\omega',\vartheta))$, with $\ell(\omega',\vartheta)$ given by Eq. (7).

The cross section

$$\frac{d\sigma}{d\Omega d\omega'} = \frac{r_e^2}{8\pi \int_{-\infty}^{\infty} d\phi\, g_X(\phi)^2} \frac{\omega' |M(\ell(\omega',\vartheta))|^2}{(k_L \cdot p)(k_L \cdot p')}, \tag{23}$$

depending on spin and polarization variables, is normalized to the incident x-ray flux ($r_e \simeq 2.8$ fm is the classical electron radius). Equation (23) is differential in the final photon momenta. The final-state electron is supposed to remain unobserved, i.e., the final electron momentum p' is integrated out and its value is fixed by Eq. (6). In the limit $a_L \to 0$, i.e., a vanishing laser field, we recover from (18) the KN matrix element and from Eq. (23) the KN cross section [46], however, both ones with the initial photon X described as a wave packet.

We emphasize the finite x-ray pulse length T_X encoded in g_X. Without g_X, the integral C_0 would diverge as $1/\ell$ for $\ell \to 0$, even after a regularization similar to Ref. [16]. This is no issue for nonlinear Compton scattering since there $\ell = 0$ implies $\omega' = 0$ [18]. Here, however, $\ell = 0$ denotes the KN line. The behavior of C_0 at $\ell = 0$ can be related to the scattering of x-ray photons during the time interval outside the laser pulse, where no laser photons are exchanged. The time integrated probability for that partial process grows $\propto T_X$ for large T_X while the probability for the scattering inside the laser pulse stays finite for finite T_L. This leads to a relative suppression of the influence of the laser pulse for large values of T_X. In Ref. [14], where laser-assisted Compton scattering was studied in a pulsed laser field combined with infinite monochromatic x-ray waves, the authors introduced a short finite observation time to fix this issue. In our approach, working with finite x-ray pulses from the beginning, we naturally obtain consistent results, where the value of T_X is related to the specific experimental conditions.

IV. PROPERTIES OF THE SPECTRUM

In the following we calculate the spectrum of laser-assisted Compton scattering numerically for a representative choice of parameters to exhibit the essential features.

A. Choice of parameters

The following numerical results are for an experiment, which could be realized when combining an XFEL (e.g., LCLS or European XFEL) with an optical laser. That means, despite of the coherence properties, the XFELs are considered as sources of short, almost monochromatic x-ray photon pulses. For the sake of definiteness we specify $\omega_X = 5$ keV for the x rays as well as an 800 nm Ti:Sapphire laser, i.e., $\omega_L = 1.55$ eV. The planned Helmholtz international beam line for extreme fields (HIBEF) [47] at the European XFEL [48] will provide such a setup. We envisage laser intensities $I \sim 10^{18}$ W/cm^2, where $a_L = 0.68\sqrt{I[10^{18}\ \mathrm{W/cm^2}]}$. The optical laser pulse length is set to $T_L = 20$ fs and the x-ray pulse length is taken as $T_X = 50$ fs (both FWHM values), in agreement with routinely achieved optical laser pulses and XFEL design [48]. For convenience we use a $\cos^2$ profile [44] for g_L and a Gaussian for g_X.

In the following we calculate the photon spectra for laser-assisted Compton scattering in the rest frame of the initial electron and focus on photon energies $\omega' = O(\mathrm{keV})$ in the vicinity of the KN line.

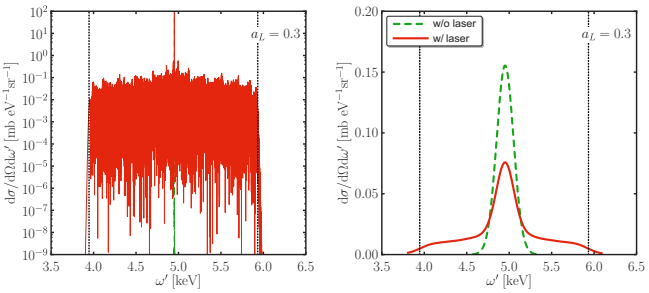

FIG. 2. (Color online) Differential cross section (left panel in a log scale) as a function of ω' for the fixed observation direction $\vartheta = 90°$ and $\varphi = 45°$ for $a_L = 0.3$. The vertical dotted lines depict the cutoff values (25), (26). The right panel shows, in a linear scale, the spectrum with 100 eV (rms Gaussian shape) resolution (red solid curve); for a comparison, the plain KN line without the laser is depicted as green dashed curve.

In an actual experiment one could employ low-energy electrons emitted from an electron gun [38]. The results from the electron rest frame can be boosted to the laboratory frame using Lorentz transformations. For low electron kinetic energies $E_{\mathrm{kin}} \ll m$, e.g., the frequencies are transformed as $\omega'_{\mathrm{lab}} \simeq \omega'[1 + \frac{v}{2}(1 + \cos\vartheta)]$, where $v = \sqrt{2E_{\mathrm{kin}}/m}$ and scattering angles close to $\vartheta = \pi/2$ transform as $\vartheta_{\mathrm{lab}} \simeq \vartheta + v$.

B. Energy spectra

The unpolarized differential cross section is exhibited in Fig. 2 as a function of the frequency ω' for a fixed observation direction $\vartheta = 90°$ and $\varphi = 45°$. The scattering angle ϑ is measured with respect to the beam axis $\boldsymbol{k}_L$; the azimuthal angle φ with respect to $\boldsymbol{\epsilon}_L$. In the left panel of Fig. 2, for $a_L = 0.3$ many side lines form a roughened plateau, where the main KN line sticks out being very narrow as compared to the width of the plateau. The plateau spans the range 4−6 keV, corresponding to the order of 1 keV/$\omega_L \sim 650$ exchanged laser photons, despite of $a_L < 1$. The right panel depicts the spectrum, averaged with a detector resolution of 100 eV, on a linear scale. While the KN line becomes broader, the plateau is clearly visible and the roughness is averaged out (red curve). Compared to Compton scattering without the laser (green dashed curve), the peak height of the Klein Nishina line is reduced to half of its value (see also the discussion in Sec. IV D).

To find the relevant multiphoton parameter for the process in Fig. 1(c) we determine the cutoff values $\ell_\pm$, beyond which the amplitude drops exponentially fast, via the stationary phase method by requiring that there are no stationary points $\phi_\star$ on the real axis, i.e., $\psi(\phi_\star) = 0$ [see Eq. (20)] has no real solutions. Abbreviating $f = g_L(\phi)\cos\phi$ we find

$$f(\phi_\star) = -\frac{\alpha_L}{2\beta_L} \pm \sqrt{\frac{\alpha_L^2}{4\beta_L^2} - \frac{\ell}{\beta_L}}, \tag{24}$$

which has no real solutions for $\phi_\star$ if (i) the term under the root becomes negative or (ii) there are no real solutions when calculating the inverse function f^{-1}. The cutoff values are

determined at maximum intensity at the center of the pulse, thus, we may set $g_L \to 1$ here and condition (ii) turns into $|f| \leqslant 1$. We find

$$\ell_- = \frac{\varkappa\xi_-}{1-\xi_-}\,, \tag{25}$$

$$\ell_+ = \begin{cases} \frac{\varkappa\xi_+}{1-\xi_+}\,, & \text{for} \quad \vartheta \leqslant \vartheta_\star\,, \\ \frac{\varkappa\xi_0}{1-\xi_0}\,, & \text{for} \quad \vartheta > \vartheta_\star \end{cases} \tag{26}$$

with

$$\xi_0 = \frac{\sin^2\vartheta\cos^2\varphi}{2-2\cos\vartheta}\,, \tag{27}$$

$$\xi_\pm = \frac{a_L^2}{2}(\cos\vartheta - 1) \pm a_L \sin\vartheta\,|\cos\varphi| \tag{28}$$

and

$$\cos\vartheta_\star = \frac{a_L^2 - \cos^2\varphi}{a_L^2 + \cos^2\varphi}\,. \tag{29}$$

For $a_L < 1$, the cutoff values are of the order $\varkappa a_L$ for most observation angles. Thus, for moderately strong laser fields and a large frequency ratio the relevant multiphoton parameter is $\varkappa a_L$. This is in severe contrast to the spontaneous process S_0 depicted in Fig. 1(b), where the multiphoton parameter is a_L [49].

C. Angular spectra

The plateau has a pronounced dependence on the azimuthal angle φ, see left panel of Fig. 3. A strong reduction of the plateau width is observed at $\varphi = 90^\circ$, i.e., perpendicularly to the laser polarization, where $\ell_+ = 0$. The broadest plateau is found close to the laser polarization direction which is perpendicular to the x-ray polarization where up to 1000 laser photons participate. The polar angle distribution (right panel) shows a forward-backward asymmetry. For large scattering angles $\vartheta > 90^\circ$ the emission with $\ell > 0$, i.e. $\omega' > \omega'_{\rm KN}$ is suppressed. The cutoff values (25), (26), depicted by dotted curves, coincide with the numerical results. From our analysis of the angular spectra we propose to choose as observation direction $\vartheta = 90^\circ$ and an azimuthal angle not too close to $\varphi = 90^\circ$, e.g., as discussed above in Fig. 2, to optimize the width of the plateau.

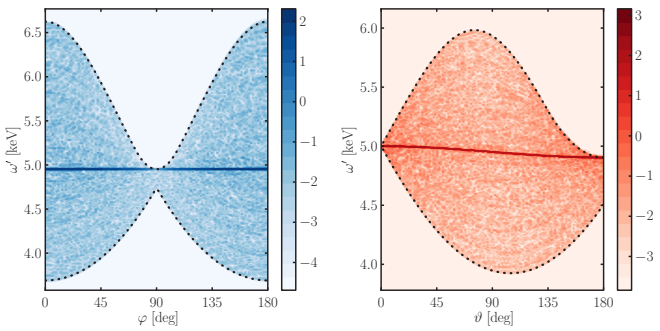

FIG. 3. (Color online) Frequency vs angle correlations of the cross section as a function of the azimuthal angle for fixed $\vartheta = 90^\circ$ (left panel) and as a function of ϑ for fixed $\varphi = 45^\circ$ (right panel) for $a_L = 0.3$. The cutoff values (25), (26) are depicted by the dotted curves. The color scale represents $\log_{10}(d\sigma/d\Omega d\omega'$ [mb eV^{-1}sr^{-1}]).

D. Energy integrated cross section

Numerically we find that the energy integrated cross section equals the KN cross section [50], i.e.,

$$\int d\omega' \frac{d\sigma}{d\Omega d\omega'} = \frac{d\sigma_{\rm KN}}{d\Omega}\,. \tag{30}$$

A qualitative argument for this behavior is provided by a classical model, where the total emitted power $\dot{E}$ is given by the Larmor formula yielding

$$\dot{E} = -\frac{e^4}{6\pi m^2}(A'_L \cdot A'_L + A'_X \cdot A'_X)\,, \tag{31}$$

where primes denote derivatives with respect to ϕ. The first term in brackets corresponds to the spontaneous emission process and the second term refers to the laser-assisted Compton scattering of x-ray photons S_{+1}. The latter part is independent of the laser intensity. Such a redistribution in phase space with marginal impact on the total probability has been found also for other laser-assisted processes [51].

To quantify the fraction of photons scattered into the side bands, in particular for the observation direction used in Fig. 2, we define the side-band cross section as that part of the spectrum which is at least by $\pm\omega_L/2$ away from $\omega'_{\rm KN}$. (A variation of the discrimination value in the range 0.25–0.75 ω_L leads to a relative uncertainty of $\leqslant 5\%$.) For small values of $\varkappa a_L \ll 1$, the side-band fraction scales as a_L^2. For larger values of a_L, the main line is weakened, see right panel in Fig. 2. (For monochromatic waves, where $g_{X,L} \to 1$, also a negative lowest-order a_L corrections to the main line has been found [8,9]). The side-band cross section increases with a_L up to $a_L \sim 0.01$, where it saturates at 30 mb sr^{-1}. This value should be compared to the corresponding KN cross section (without the laser) of 39 mb sr^{-1}, proving that a large fraction of the photons is emitted into the side bands.

E. Polarization

Due to the nonlinear mixing of optical laser photons with the incident x-ray photon the polarization of the photon X' is rotated as compared to Compton scattering without the laser. The rotation angle is frequency dependent. This rotation can be quantified experimentally by measuring the Stokes parameter P_2, which we calculate as $P_2 = (w_{45^\circ} - w_{135^\circ})/(w_{45^\circ} + w_{135^\circ})$, where w_χ denotes the triple differential cross section of photons with their polarization vector having an angle of χ with respect to the scattering plane. For instance, for the observation angles of Fig. 2 the photon X' is polarized perpendicular to the scattering plane without the laser, which means $P_2 = 0$. This result is changed in laser-assisted Compton scattering. In Fig. 4 the Stokes parameter P_2 is exhibited as a function of ω' for $a_L = 0.3$. The value of P_2 is zero at the KN line and increases with increasing distance from it, i.e., in the region where more laser photons are involved. The maximum value of P_2 corresponds to a rotation angle of 5° towards $\boldsymbol{k}_L$. In the classical picture, the figure-eight orbit in the laser field has a component in the directions of $\boldsymbol{k}_L$, which is transferred to the polarization of the photon X'.

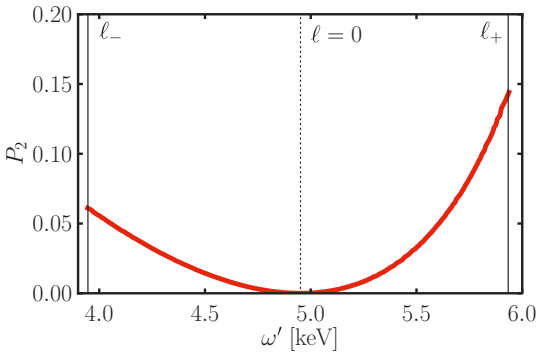

FIG. 4. (Color online) Rotation of the polarization of the scattered photon, quantified via the Stokes parameter P_2 as a function of ω' for the same observation direction as in Fig. 2.

The energy dependent polarization rotation can be used to identify unambiguously the final-state photons emerging from the multiphoton process.

V. DISCUSSION AND SUMMARY

A clear and easily observable signature of laser-assisted Compton scattering of x-ray photons is provided by the side lines accompanying the main Klein-Nishina line forming a broad plateau. Due to the difference of scales of the photon energies of x-ray and optical laser, nonlinear effects are strongly enhanced as compared to the spontaneous emission of radiation in a pure laser field. The relevant multiphoton parameter is $\varkappa a_L$, which can be large even for laser fields with intensities of the order of $10^{18}\mathrm{W/cm}^2$. The optimal conditions to observe the side-band plateau with an x-ray camera are achieved for $a_L \lesssim 1$. Such intensities are achieved routinely with a 200 TW laser in relatively large spot sizes of $w_0 = O(100\ \mu\mathrm{m})$ and pulse lengths of $T_L = 20$ fs. We do not expect that spatially inhomogeneous laser spots influence the cutoff values since they are sensitive to the maximum laser intensity in the spatiotemporal profile of the pulse. However, the shape of the plateau will certainly change. The optical photons emerging from spontaneous emission process, i.e., the nonlinear Compton process exhibited in Fig. 1(b), can be efficiently filtered out by a thin foil which is otherwise transparent for x rays.

A very useful signal for the nonlinear frequency mixing is the frequency-dependent rotation of the polarization of the final-state photons. The polarization can be measured by using x-ray polarizers. A polarization purity of the order of 10^{-10} has been achieved recently [52]. The technique of a polarization veto can be used to shield the plain KN photons (arising for unsynchronized X and L pulses) or shield the $\ell = 0$ KN-like photons. For optimal conditions, the x-ray pulse length T_X and the laser pulse length T_L should be of the same order of magnitude. The synchronization of optical and x-ray pulses to the level of femtoseconds has been achieved experimentally [53], approaching the subfemtosecond level [54]. Numerically, the spectra are insensitive to a temporal offset between the two pulses of the order of a few femtoseconds.

A slight misalignment of the x-ray and laser beams due to axis offsets or focusing effects does not lead to qualitatively new effects: The Oleinik resonances [7] for nonparallel beams (see, e.g., Refs. [55–58]) are suppressed by the large frequency ratio $\varkappa$ and for a small angular misalignment $\Theta \ll 1$ between the x-ray and laser beams. A slight misalignment of the polarizations, $\boldsymbol{\epsilon}_X \cdot \boldsymbol{\epsilon}_L \neq 0$, causes laser-intensity-dependent modifications of the total cross section of the order $O(\boldsymbol{\epsilon}_X \cdot \boldsymbol{\epsilon}_L) \ll 1$.

Such experiments can be performed at LCLS or at the European XFEL combining the x-ray facility with an optical laser system, e.g., as planned in HIBEF [47]. One could employ low-energy electrons emitted from an electron gun as in the experiment [38]. However, the electron energy cannot be too low since low-energy electrons are expelled from high-intensity regions due to the ponderomotive force. We found numerically that for electron kinetic energies as low as $E_{\mathrm{kin}} = 500$ eV the electrons can penetrate the focus and the maximum deflection angle is below 0.8°. This is due to the fact that the transverse ponderomotive force, which is responsible for the deflection, is proportional to the gradient of the laser intensity and scales as $\propto a_L^2/w_0$, where a_L is rather small and the laser spot size w_0 is large. Consequently, electrons with kinetic energies of a few hundred eV are suitable for such experiments.

In conclusion, studying the laser-assisted Compton scattering of x rays will significantly advance our understanding of strong-field QED scattering processes in the $O(10^3)$ multiphoton regime.

ACKNOWLEDGMENTS

The authors are grateful to T. E. Cowan and R. Sauerbrey for the inspiring collaboration and discussions on future experiments at HIBEF. D.S. acknowledges stimulating discussions with S. Fritzsche, A. Surzhykov, and V. G. Serbo.

APPENDIX: LIMIT OF INFINITE MONOCHROMATIC PLANE WAVES

In this Appendix we discuss briefly the limit of infinite monochromatic plane waves (IPW), $T_X, T_L \to \infty$. In this case, characterized by $g_{L,X} \to 1$, the integral in the exponents of the functions C_n, Eq. (19), is given by

$$\int d\phi\, \psi_{\mathrm{IPW}}(\phi) = \ell\phi + \alpha_L \sin\phi + \frac{\beta_L}{2}\phi + \frac{\beta_L}{4}\sin 2\phi. \quad \text{(A1)}$$

Owing to the periodicity of the monochromatic field, the integrand of the C_n can be expanded in a discrete Fourier series, excluding the nonperiodic terms in (A1), such that the integrals C_n turn into a sum over discrete partial amplitudes. For instance, for C_0 we find

$$C_0^{\mathrm{IPW}} = \sum_{N=-\infty}^{\infty} 2\pi\delta(\ell - N + \beta_L/2) J_N(\alpha_L, \beta_L) \quad \text{(A2)}$$

with amplitudes

$$J_N(\alpha_L, \beta_L) = \sum_{s=-\infty}^{\infty} J_{N-2s}(-\alpha_L) J_s(-\beta_L/4) \quad \text{(A3)}$$

and the Bessel functions J_N. Similar relations can be found for all integrals C_n^{IPW}. Thus, in the limit of infinite plane waves the variable ℓ becomes a discrete $\ell_N = N - \beta_L/2$, with integer

values of N, due to $\delta(\ell - N + \beta_L/2)$. The term $\beta_L/2$ can be absorbed into the electron momenta leading to the occurrence of the field-dressed quasi-momentum

$$\tilde{p} = p + \frac{m^2 a_L^2}{4k_L \cdot p} k_L \,, \tag{A4}$$

and similarly for p'. The formal energy momentum conservation (5) turns into

$$\tilde{p} + k_X + N k_L = \tilde{p}' + k' \,, \tag{A5}$$

where N can be considered as number of laser photons exchanged during the scattering process, as pointed out, e.g., in [19,41] for nonlinear Compton scattering. Solving (A5) for the frequency ω' gives

$$\omega'_N(\vartheta) = \frac{\omega_X + N\omega_L}{1 + \left(\frac{\omega_X + N\omega_L}{m} + \frac{a_L^2}{4}\right)(1 - \cos\vartheta)} \,, \tag{A6}$$

i.e. discrete frequencies ω'_N with an intensity dependent redshift quantified by the term $a_L^2/4$ in the denominator [11].

Integrating over $d\ell$ in (17) and exploiting the delta distributions in the functions C_n^{IPW}, the amplitude M, Eq. (18), becomes a sum of discrete partial amplitudes

$$M_{\mathrm{IPW}} = \sum_N M_N \,. \tag{A7}$$

The same is true for the cross section

$$\frac{d\sigma_{\mathrm{IPW}}}{d\Omega} = \sum_N \frac{d\sigma_N}{d\Omega} \,, \tag{A8}$$

as known from the literature, e.g., [8,9,11]. The dependence on ω' in (23) is replaced by a sum over discrete values of N. This shows that our results for pulsed plane waves, in particular (17), (18), and (23), contain also the known case of infinite plane waves in the proper limit.

[1] A. H. Compton, Phys. Rev. **21**, 483 (1923).
[2] F. Ehlotzky, J. Phys. B **20**, 2619 (1987).
[3] A. Weingartshofer, J. K. Holmes, G. Caudle, E. M. Clarke, and H. Krüger, Phys. Rev. Lett. **39**, 269 (1977).
[4] R. Taïeb, A. Maquet, and M. Meyer, J. Phys. Conf. Ser. **141**, 012017 (2008).
[5] E. S. Sarachik and G. T. Schappert, Phys. Rev. D **1**, 2738 (1970).
[6] A. Di Piazza, C. Müller, K. Z. Hatsagortsyan, and C. H. Keitel, Rev. Mod. Phys. **84**, 1177 (2012).
[7] V. P. Oleĭnik, Sov. Phys. JETP **26**, 1132 (1968).
[8] R. Guccione-Gush and H. P. Gush, Phys. Rev. D **12**, 404 (1975).
[9] A. I. Akhiezer and N. P. Merenkov, Sov. Phys. JETP **61**, 41 (1985).
[10] A. K. Puntajer and C. Leubner, Phys. Rev. A **40**, 279 (1989).
[11] F. Ehlotzky, J. Phys. B **22**, 601 (1989).
[12] V. C. Zhukovskii and N. S. Nikitina, Sov. Phys. JETP **37**, 595 (1973).
[13] V. N. Baier, V. M. Katkov, and V. M. Strakhovenko, *Electromagnetic Processes at High Energies in Oriented Single Crystals* (World Scientific, Singapore, 1998).
[14] V. N. Nedoreshta, S. P. Roshchupkin, and A. I. Voroshilo, Laser Phys. **23**, 055301 (2013).
[15] N. B. Narozhnyi and M. S. Fofanov, JETP **83**, 14 (1996).
[16] M. Boca and V. Florescu, Phys. Rev. A **80**, 053403 (2009).
[17] T. Heinzl, D. Seipt, and B. Kämpfer, Phys. Rev. A **81**, 022125 (2010).
[18] D. Seipt and B. Kämpfer, Phys. Rev. A **83**, 022101 (2011).
[19] F. Mackenroth and A. Di Piazza, Phys. Rev. A **83**, 032106 (2011).
[20] K. Krajewska and J. Z. Kamiński, Phys. Rev. A **85**, 062102 (2012).
[21] D. Seipt and B. Kämpfer, Phys. Rev. A **88**, 012127 (2013).
[22] T. Heinzl, A. Ilderton, and M. Marklund, Phys. Lett. B **692**, 250 (2010).
[23] T. Nousch, D. Seipt, B. Kämpfer, and A. I. Titov, Phys. Lett. B **715**, 246 (2012).
[24] K. Krajewska, C. Müller, and J. Z. Kamiński, Phys. Rev. A **87**, 062107 (2013).
[25] C. Kohlfürst, M. Mitter, G. von Winckel, F. Hebenstreit, and R. Alkofer, Phys. Rev. D **88**, 045028 (2013).
[26] A. Ilderton, P. Johansson, and M. Marklund, Phys. Rev. A **84**, 032119 (2011).
[27] D. M. Volkov, Z. Phys. **94**, 250 (1935).
[28] A. I. Voroshilo and S. P. Roshchupkin, Laser Phys. **7**, 466 (1997).
[29] K. Krajewska and J. Z. Kamiński, Phys. Rev. A **85**, 043404 (2012).
[30] S. Augustin and C. Müller, Phys. Rev. A **88**, 022109 (2013).
[31] A. I. Voroshilo, S. P. Roshchupkin, and V. N. Nedoreshta, in *Proceedings of the 12th International Conference on Laser and Fiber-Optical Networks Modeling* (IEEE, New York, 2013), p. 32.
[32] J. Herrmann and V. C. Zhukovskii, Ann. Phys. (Leipzig) **482**, 349 (1972).
[33] H. Hu and C. Müller, Phys. Rev. Lett. **107**, 090402 (2011).
[34] There are corrections to that process of the order of a_X^2 when arranging the expansion of Fig. 1(a) according to the energy-momentum balance $\ell k_L + p = p' + k'$ [32].
[35] L. S. Brown and T. W. B. Kibble, Phys. Rev. **133**, A705 (1964).
[36] N. B. Narozhnyi, A. I. Nikishov, and V. I. Ritus, Sov. Phys. JETP **20**, 622 (1965).
[37] C. Harvey, T. Heinzl, and A. Ilderton, Phys. Rev. A **79**, 063407 (2009).
[38] T. J. Englert and E. A. Rinehart, Phys. Rev. A **28**, 1539 (1983).
[39] C. Bula *et al.*, Phys. Rev. Lett. **76**, 3116 (1996).
[40] S.-Y. Chen, A. Maksimchuk, and D. Umstadter, Nature (London) **396**, 653 (1998).
[41] C. Harvey, T. Heinzl, A. Ilderton, and M. Marklund, Phys. Rev. Lett. **109**, 100402 (2012).
[42] A. Ilderton, Phys. Rev. Lett. **106**, 020404 (2011).
[43] E. Lötstedt and U. D. Jentschura, Phys. Rev. Lett. **103**, 110404 (2009).
[44] D. Seipt and B. Kämpfer, Phys. Rev. D **85**, 101701 (2012).
[45] F. Mackenroth and A. Di Piazza, Phys. Rev. Lett. **110**, 070402 (2013).
[46] O. Klein and Y. Nishina, Z. Phys. **52**, 853 (1929).
[47] "The HIBEF project", www.hzdr.de/hgfbeamline/
[48] "The European XFEL project", http://www.xfel.eu/

[49] V. I. Ritus, J. Sov. Laser Res. **6**, 497 (1985).
[50] W. B. Berestetzki, E. M. Lifschitz, and L. P. Pitajewski, *Relativistische Qantentheorie*, Lehrbuch der Theoretischen Physik, Vol. IV (Akademie Verlag, Berlin, 1980).
[51] E. Lötstedt, U. D. Jentschura, and C. H. Keitel, Phys. Rev. Lett. **101**, 203001 (2008).
[52] B. Marx *et al*., Phys. Rev. Lett. **110**, 254801 (2013).
[53] F. Tavella, N. Stojanovic, G. Geloni, and M. Gensch, Nat. Photon. **5**, 162 (2011).
[54] M. Schultze *et al*., Science **328**, 1658 (2010).
[55] A. Hartin, Ph.D. thesis, University of London, 2006.
[56] A. I. Voroshilo and S. P. Roshchupkin, Laser Phys. Lett. **2**, 184 (2005).
[57] A. I. Voroshilo, S. P. Roshchupkin, and V. N. Nedoreshta, Laser Phys. **21**, 1675 (2011).
[58] V. N. Nedoreshta, A. I. Voroshilo, and S. P. Roshchupkin, Phys. Rev. A **88**, 052109 (2013).